Report

Current Biology

# Natural Variation in *plep-1* Causes Male-Male Copulatory Behavior in *C. elegans*

## Highlights

- Wild isolates of *C. elegans* vary in a male-male mating behavior
- In some isolates, males deposit copulatory plugs on each other's excretory pores
- A mutation in a conserved gene renders pores attractive or receptive to matings
- Excretory pore plugging may be a side effect of mating system evolution

## Authors

Luke M. Noble, Audrey S. Chang, Daniel McNelis, ..., Matthew Phillips, Tangirul Islam, Matthew V. Rockman

## Correspondence

mrockman@nyu.edu

## In Brief

Noble et al. identify the genetic cause of natural variation in male-male copulatory behavior in *C. elegans*. Males homozygous for a loss-of-function mutation in one member of a highly conserved gene family have excretory pores that are attractive or receptive to mating by other males. The gene, *plep-1*, is expressed in the excretory cell.

## Accession Numbers

GSE68351

Noble et al., 2015, Current Biology *25*, 2730–2737
October 19, 2015 
http://dx.doi.org/10.1016/j.cub.2015.09.019

CellPress

CellPress

Current Biology
Report

# Natural Variation in *plep-1* Causes Male-Male Copulatory Behavior in *C. elegans*

Luke M. Noble,[1] Audrey S. Chang,[1] Daniel McNelis,[1] Max Kramer,[1] Mimi Yen,[1] Jasmine P. Nicodemus,[1] David D. Riccardi,[1] Patrick Ammerman,[1] Matthew Phillips,[1] Tangirul Islam,[1] and Matthew V. Rockman[1,*]
[1]Department of Biology and Center for Genomics & Systems Biology, New York University, 12 Waverly Place, New York, NY 10003, USA
*Correspondence: mrockman@nyu.edu
http://dx.doi.org/10.1016/j.cub.2015.09.019

## SUMMARY

**In sexual species, gametes have to find and recognize one another. Signaling is thus central to sexual reproduction and involves a rapidly evolving interplay of shared and divergent interests [1–4]. Among *Caenorhabditis* nematodes, three species have evolved self-fertilization, changing the balance of intersexual relations [5]. Males in these androdioecious species are rare, and the evolutionary interests of hermaphrodites dominate. Signaling has shifted accordingly, with females losing behavioral responses to males [6, 7] and males losing competitive abilities [8, 9]. Males in these species also show variable same-sex and autocopulatory mating behaviors [6, 10]. These behaviors could have evolved by relaxed selection on male function, accumulation of sexually antagonistic alleles that benefit hermaphrodites and harm males [5, 11], or neither of these, because androdioecy also reduces the ability of populations to respond to selection [12–14]. We have identified the genetic cause of a male-male mating behavior exhibited by geographically dispersed *C. elegans* isolates, wherein males mate with and deposit copulatory plugs on one another's excretory pores. We find a single locus of major effect that is explained by segregation of a loss-of-function mutation in an uncharacterized gene, *plep-1*, expressed in the excretory cell in both sexes. Males homozygous for the *plep-1* mutation have excretory pores that are attractive or receptive to copulatory behavior of other males. Excretory pore plugs are injurious and hermaphrodite activity is compromised in *plep-1* mutants, so the allele might be unconditionally deleterious, persisting in the population because the species' androdioecious mating system limits the reach of selection.**

## RESULTS AND DISCUSSION

Gems and Riddle found that males of the Australian wild isolate AB2, maintained in male-only populations, deposit copulatory plugs on one another's excretory pores (Figures 1A and 1B) [10]. Most *C. elegans* strains, including the Hawaiian isolate CB4856, do not exhibit this behavior, although it also present and variable in the androdioecious *C. briggsae* [6]. The excretory system, which functions in osmoregulation, is essential for development and viability [15], and we found that pore plugs impinge on male function. Relative to their genetically identical brothers, plugged *C. elegans* adult males lived less long (Cox proportional hazard regression coefficient and standard error: $-0.654 \pm 0.189$, $p = 0.0005$; see Experimental Procedures and Figure S1) and had lower mating success well before differences in mortality were apparent (Fisher's exact test, $p = 0.0008$).

To dissect the genetic causes of excretory pore plugging, we intercrossed AB2 and CB4856 (each carrying a male-generating *him-5* mutation) and created recombinant inbred lines (RILs) from $F_2$ hermaphrodites by selfing for ten generations. We genotyped 82 RILs at 157 markers and scored their copulatory plugs in 4-day, 40-male assays (Supplemental Information). RILs varied in the frequency of plugs deposited on excretory pores (Plep, plugged excretory pore) and also in frequency of plugs placed elsewhere on males' bodies (Plob, plugged on body), which occurs rarely in the parental strains (Movies S1 and S2). The phenotypes exhibit transgressive segregation, with many RILs showing higher plug frequencies than the parental strains (Figure 1C), and they implicate different genomic regions (Figure 1D).

A major-effect QTL on chromosome II largely discriminates between strains with some excretory-pore plugging and those with none (Figures 1C and 1D), while the residual variation in plug frequency among strains is genetically complex, with significant QTLs on chromosomes II, III, and V. Plug deposition elsewhere on the body maps to chromosomes IV and X. However, after conditioning on the major-effect Plep QTL, residual variance for that phenotype is correlated with the variance in Plob (correlation of strain effects is 0.36, $p = 0.00089$), suggesting shared etiology. All QTL effects are as predicted by parental differences: AB2 alleles at the four Plep QTLs increase excretory pore plugging and CB4856 alleles at the two Plob QTLs increase male body plugging. However, transgressive segregation implies that additional undetected loci act in the reciprocal directions.

The Plep phenotype could be due to increased copulatory activity or to increased attractiveness or receptivity of Plep males [10]. To distinguish between these possibilities, we introgressed a defective *plg-1* allele into QG71, the most highly Plep RIL, rendering these animals incapable of making copulatory plugs [9]. We then assayed populations comprising 10 *plg-1*$^-$ RIL males and 30 GFP-marked CB4856 males. After 4 days, an

 

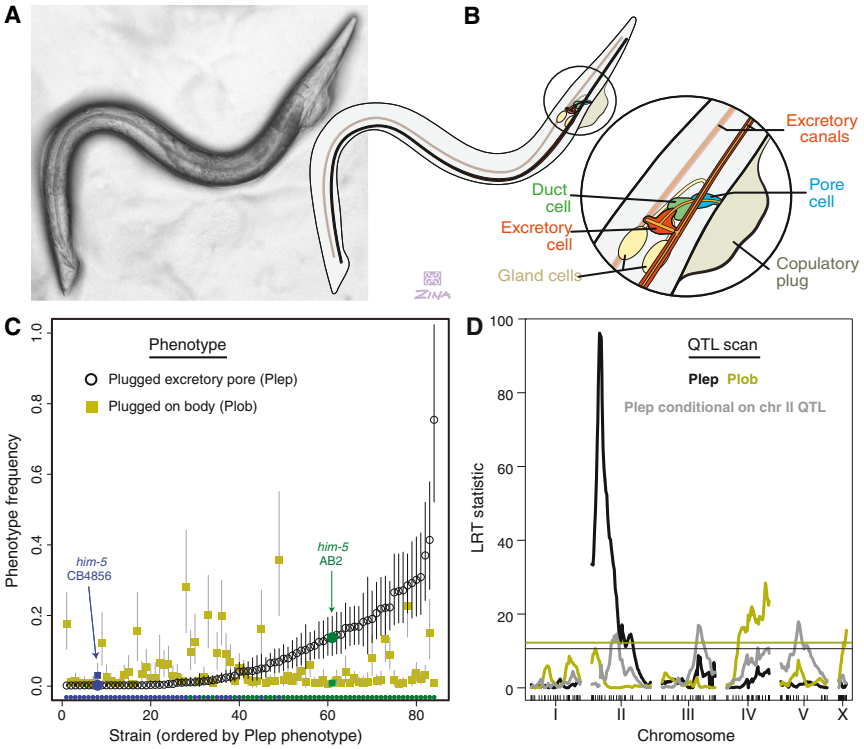


**Figure 1. Excretory System Anatomy and the Genetic Architecture of Excretory Pore Plugging**

(A) A male worm with a copulatory plug on its excretory pore (QG71, right lateral view).

(B) Schematic of the excretory system. Paired bilaterally symmetric canals are drained through the excretory, duct, and pore cells, immediately posterior and ventral to the pharyngeal bulb. The function of the gland cells is unknown.

(C) Ectopic copulatory plugging exhibits transgressive segregation. Of the 82 recombinant inbred lines, ordered by Plep phenotype, many have higher Plep and Plob frequencies than either parental strain (blue and green). The plotted values and prediction intervals are derived from a mixed-effect generalized linear model (see Experimental Procedures). Colors at the bottom represent strain genotype at the major-effect Plep QTL.

(D) QTL mapping of ectopic copulatory plugging in the recombinant inbred lines. Single QTL scans for excretory pore (black) and body (gold) plugging show one and two significant linkages. After conditioning on the major chromosome II QTL, three additional Plep QTL are significant (gray). Horizontal lines show permutation-based thresholds for genome-wide significance at p = 0.05.

average of 5.4 *plg-1*$^{-}$ males, and none of the CB4856 males, had received excretory pore plugs, indicating that males of the non-Plep strain CB4856 readily copulate with the excretory pores of other males and that pore attractiveness or receptivity underlies the Plep phenotype.

The major-effect chromosome II QTL is specific to the Plep phenotype and thus is predicted to confer pore attractiveness to animals that carry the AB2 allele. We assayed genetically heterogeneous $F_2$ male populations from a cross of AB2 and CB4856 and found that genetic markers closely linked to the QTL cosegregated, in a recessive pattern, with receipt of excretory pore plugs ($p < 10^{-15}$ for linkage, $p < 10^{-4}$ for dominance; Figure 2A; Supplemental Information).

The attractiveness of Plep males is modulated by the presence of hermaphrodites. QG71 exhibits reduced Plep when a single vulvaless hermaphrodite is present among males ($p < 10^{-11}$; Figure 2B), and aqueous extract from a hermaphrodite culture is sufficient to decrease male-male copulation ($p = 0.015$; Figure 2C; Supplemental Information).

Water-soluble ascaroside pheromones mediate communication in nematode populations and are candidate factors governing male attractiveness [16, 17]. To test whether ascarosides underlie the Plep phenotype, we introgressed *dhs-28(hj8)*, a mutation that abrogates synthesis of the short-chain ascaroside pheromones [18], from the N2 lab background into QG71. In parallel, we introgressed the wild-type N2 genome into the same region to make *dhs-28*$^{+}$ control strains. Pheromone-defective males exhibited slightly elevated Plep rates ($p = 9.4 \times 10^{-4}$; Figure 2D; Supplemental Information), indicating that pheromonal communication is not required for pore attractiveness, and wild-type signaling discourages plug receipt.

We attempted to Mendelize the chromosome II QTL by introgressing it from AB2 into the CB4856 background. Using visible marker mutations, we narrowed the Plep-conferring interval (Figure S2) to 27 kb, minimally defined by near-isogenic lines (NILs) QG1448 and QG1451 (Supplemental Information). The interval behaves as a recessive Mendelian locus (Figure 2E; Supplemental Information) and contains ten protein-coding genes (Figure 2F).

We sequenced the genomes of AB2 and CB4856, identifying 217 segregating variants in the NIL-defined QTL interval, and next employed association mapping to prioritize variants. Genotypes were called at the 217 positions from Illumina sequencing of 9 additional wild isolates capable of making copulatory plugs (Supplemental Information). One strain, PB306, exhibits a Plep phenotype similar to AB2 and is nearly identical across the interval, while the others exhibit diverse haplotypes and little or no Plep (Supplemental Information). Of the 217 variants, 5 are perfectly Plep-associated across the 11 strains (Figure 2F), including 3 nonsynonymous polymorphisms in two genes, *Y52E8A.4* and *Y52E8A.6*.

A *Mos1* transposon-insertion allele of *Y52E8A.6* complemented the NIL QG1448 ($p = 0.79$), but a *Y52E8A.4* insertion allele failed to complement ($p < 10^{-9}$; Figure 2G; Supplemental Information). *Y52E8A.4* carries a single variant in AB2 associated with Plep, a V > D replacement at position 278, which is predicted to fall within a conserved transmembrane helix and be highly damaging to protein function.

Knock-down of *Y52E8A.4* by feeding RNAi to L4 males caused QG1451, the non-Plep NIL, to exhibit excretory pore plugging ($p < 10^{-9}$; Figure 2H; Supplemental Information). RNAi in the CB4856 background also induced excretory pore plugging

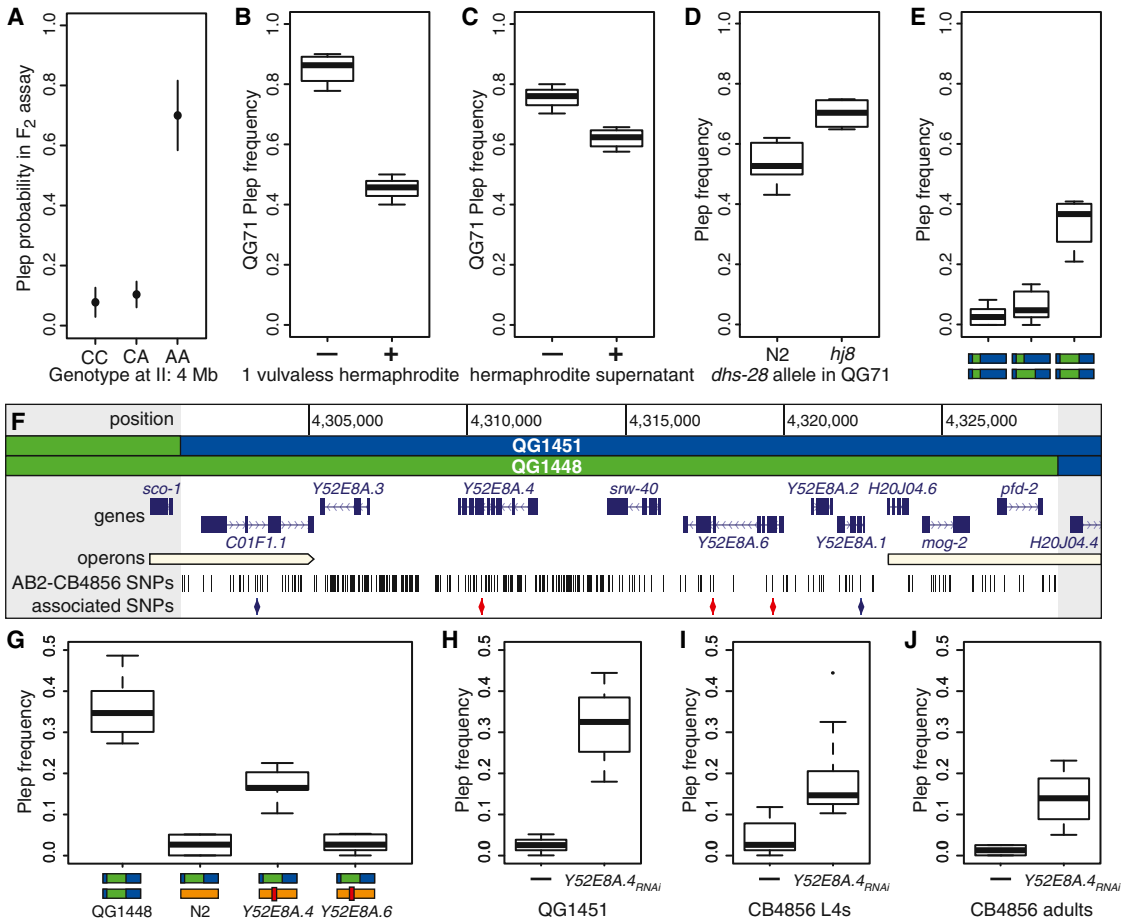


**Figure 2. Identification of *plep-1***

(A) The Chr II QTL confers recessive receptivity to excretory pore plugs in heterogeneous $F_2$ population assays. Proportions of Plep males and their binomial confidence intervals are plotted by genotype at a QTL-linked marker (C for the CB4856 allele, A for AB2).

(B and C) The frequency of Plep QG71 males is significantly reduced by the presence of a single vulvaless hermaphrodite (B) and by aqueous supernatant from hermaphrodites (C).

(D) Excretory pore plugging is not mediated by ascaroside pheromones. QG71 males with an introgression of the *dhs-28(hj8)* loss-of-function allele are plugged at higher rates than those with a matched N2 introgression.

(E and F) A 27 kb interval defined by NILs behaves as a recessive locus. Strains QG1451, QG1448, and their $F_1$ are depicted as bars representing chromosome II (E), with CB4856 DNA in blue and AB2 DNA in green, as in (F), which details the NIL-defined interval. The interval encompasses 10 protein-coding genes and 217 AB2-CB4856 nucleotide variants, of which 5 perfectly associate with Plep phenotype across 11 wild strains (blue, synonymous or intronic; red, non-synonymous).

(G) In complementation tests for *Mos1*-insertion mutants of *Y52E8A.4* and *Y52E8A.6* (N2 background: orange), *Y52E8A.4* fails to complement the Plep NIL QG1448.

(H–J) RNAi against *Y52E8A.4* induces headplugging when administered to L4 males of non-Plep NIL QG1451 (H) and CB4856 *him-5* (I) and to CB4856 *him-5* adult males (J).

($p = 10^{-7}$; Figure 2I), though at a lower level than in QG1451 ($p = 0.006$). Moreover, RNAi administered to adult CB4856 males was also effective ($p = 2 \times 10^{-5}$; Figure 2J), implying that Plep is independent of any role for *Y52E8A.4* in development and that wild-type function involves rapid protein turnover. We assigned the name *plep-1* to *Y52E8A.4*.

A *plep-1* transcriptional reporter was expressed consistently only in the excretory cell in both males and hermaphrodites (Figures 3A and 3B). The excretory cell comprises bilaterally symmetric canals and a cell body ventral to the terminal pharyngeal bulb, connected to the excretory pore by a duct cell (Figure 1B). Pore, duct, and excretory gland cells all fail to express $p_{plep\text{-}1}$::GFP. We hypothesize that alteration of excretory cell function through loss of *plep-1* activity might render the chemical milieu of the excretory pore more attractive to other males or the pore more accessible to intromission.

*plep-1* is one of 16 paralogs in *C. elegans*, part of a recurrent gene-family expansion extending across rhabditid phylogeny (Figure 3C). These genes have no known function but share a Major Facilitator Superfamily-like domain with a single-copy ortholog, *MFSD11*, in flies and mammals. The domain also occurs in a more distantly related worm gene, *unc-93*, and its orthologs in other species. UNC-93 is a presumed regulatory component of a TWIK (Tandem of P-domains in a Weakly Inward rectifying $K^+$ channel) complex [19], and PLEP-1 and its paralogs are inferred to have similar roles. TWIK channels have also undergone

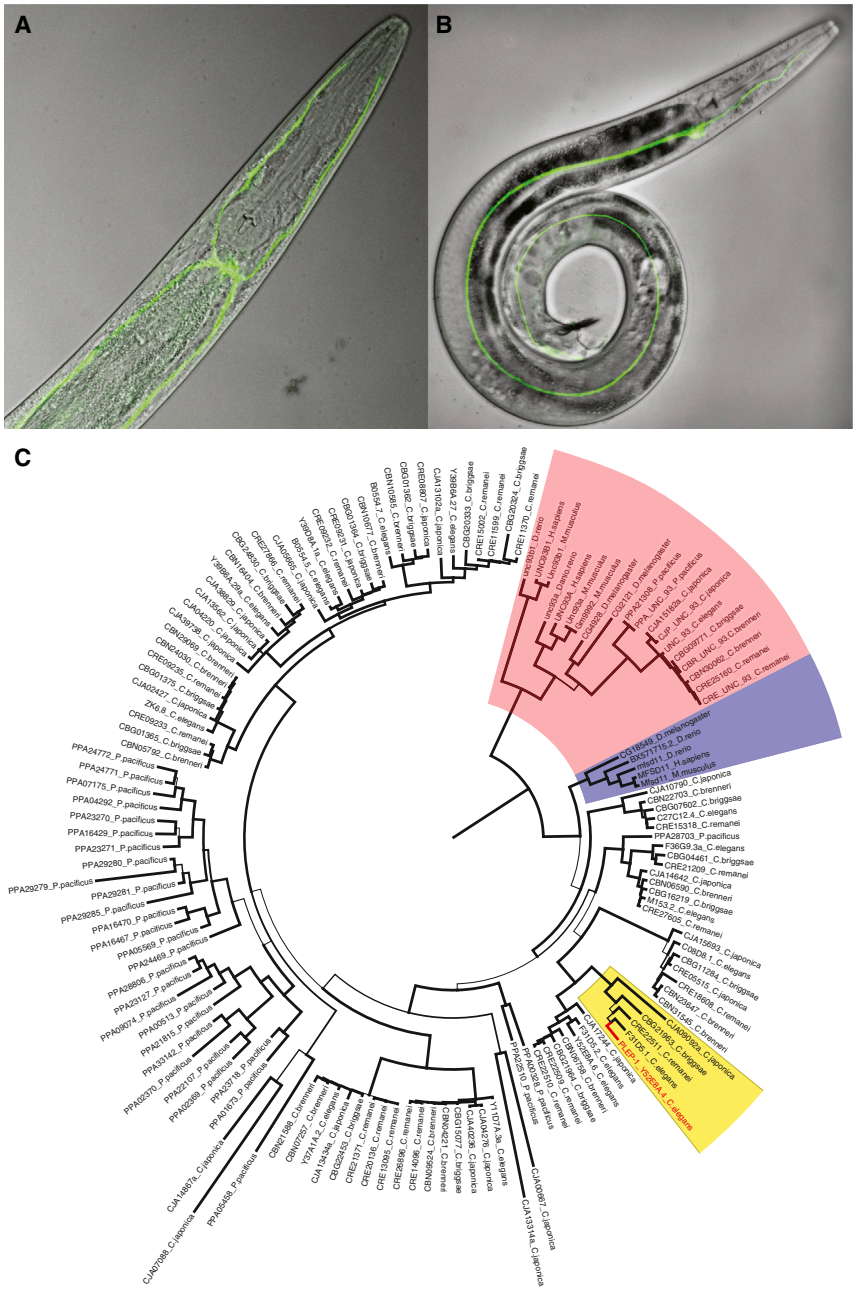


**Figure 3. *plep-1* Expression and Phylogeny**

(A) Maximum intensity projection along the dorsoventral axis showing $p_{plep-1}$::GFP expression in the excretory cell body, just posterior to the terminal pharyngeal bulb, and symmetric canals in a young adult hermaphrodite.

(B) Lateral view of a young adult male. In addition to consistent expression in the excretory cell, fluorescence in two dorsal cells in the male tail, shown here, was observed inconsistently.

(C) Phylogeny for UNC-93 domain (IPR010291) homologs. UNC-93, MFSD11, and PLEP-1 clades are highlighted (red, blue, and yellow). Unboxed genes are MFSD11 paralogs in *Caenorhabditis* and *Pristionchus* nematodes.

gene-family expansions in rhabditids, with 47 genes in the *C. elegans* genome.

Few genes show altered expression in *plep-1* mutant whole young adult hermaphrodites (Supplemental Information). Of 46 genes differentially expressed between N2 and a *plep-1* Mos1 insertion line (false discovery rate < 0.1), the two most significant are implicated in neurotransmitter biosynthesis or activity (see Supplemental Experimental Procedures) and a third, *unc-64* (syntaxin), is expressed in neurons and secretory cells including the excretory gland cells [20]. Gene set enrichment analysis identified six ontology terms overrepresented in genes with lower expression in the *plep-1* mutant ($p < 0.005$, FDR < 0.1), including aromatic amino acid metabolism, neuropeptide Y receptor activity, and a large group of mostly unstudied genes annotated by homology with transmembrane transport. While causally ambiguous, these associations are consistent with the view that loss of *plep-1* function might subtly alter the excreted small-molecule profile.

A survey of 55 wild isolates from around the world revealed that the derived 278D allele occurs in strains from Australia, Western North America, and Chile (Supplemental Information). Sets of isolates from localities in Santa Barbara, Salt Lake City, and Adelaide were polymorphic, including an instance of polymorphism among worms inhabiting a single piece of fruit. None of 15 strains from Europe, 4 from Africa, or 4 from the Azores carried the D allele. We assayed a subset of *plg-1*$^{+}$ isolates in our standard 40-worm assays. Among these strains, 278D is necessary but not sufficient for a strong Plep phenotype (Supplemental Information), indicating that genetic background affects plugging, consistent with our findings in the RILs (Figure 1C). Further, at least one isolate carrying 278D also carries a loss-of-function mutation in *plg-1*, and so is incapable of depositing copulatory plugs.

A role for male-male competition in evolution of excretory pore plugging, whether through direct injury to the plug recipient or through distraction of rival males in mating clumps, is unlikely due to the rarity of unrelated males in natural populations [9]; consistent with this, *C. briggsae* males deposit plugs on their own excretory pores [6]. Alternatively, resource-dependent male-male copulation could serve to attract receptive hermaphrodites, alleviating sperm-limited fecundity and reinforcing habitat quality cues. Given male scarcity and the low frequency of outcrossing seen in wild *C. elegans* populations [21, 22], selection on male function is expected to be a weak force in androdioecious mating systems, however. With hermaphrodite fitness generally maximized by early-life selfing, and multiple examples

of hermaphrodites eschewing male attention [6, 23, 24], a role in sexual signaling conferring a net benefit to hermaphrodites also appears unlikely.

More credibly, excretory pore plugging is compatible with mutation accumulation, due to relaxed selection on male function, or sexual antagonism, favoring alleles beneficial to hermaphrodites despite harm to males. The sexual antagonism model predicts that loss of *plep-1* function benefits hermaphrodites, while the mutation accumulation model predicts that it is neutral. We measured hermaphrodite activity, a proxy for viability and a component of fitness, as a function of *plep-1* genotype under taxing hypoosmotic conditions of starvation in water. Mutants for genes expressed in the excretory system, including TRP channel *gtl-1* and aquaporin *aqp-8*, show compromised osmotic homeostasis under similar conditions [25, 26]. We found significantly reduced activity for multiple *plep-1* loss-of-function alleles (Figure S3; Supplemental Information; generalized linear mixed model, genotype effect $p < 1 \times 10^{-12}$ after 24 hr in $H_2O$).

Although the possibility that the *plep-1* mutation might benefit hermaphrodites under other conditions cannot be excluded, and the ecological relevance of extended exposure to water is unknown, the deleterious effect of *plep-1(V278D)* on hermaphrodite activity weighs against mutation accumulation impinging solely on male function. These data instead suggest that the allele might be unconditionally deleterious for both sexes. The evolution of androdioecy, in addition to changing selection on male function, has reduced *C. elegans*' effective population size and recombination rate, such that deleterious mutations are less likely to be eliminated and more likely to hitchhike in linkage with beneficial alleles [5, 13, 14, 27, 28].

Though ascarosides underlie the attractive nature of hermaphrodite secretions [29], increasing evidence points to alternative mechanisms of mate attraction [30–32] and retention [6]. Although the worm's excretions are not well understood, our data suggest a role for *plep-1* in either the excreted chemical profile or in excretory system homeostasis, such that loss of function causes the male excretory pore to resemble the vulval microenvironment.

## EXPERIMENTAL PROCEDURES

### RIL Construction and Genotyping

We generated recombinant inbred lines from a cross of QX1199 (*him-5 (e1490)* > CB4856) males and QG5 (*him-5 (e1490)* > AB2) hermaphrodites. We singled 140 $F_2$ L4 hermaphrodites and inbred these through 10 generations of selfing, after which the 98 surviving lines were frozen. We genotyped 82 RILs at 157 SNPs by GoldenGate assay at the University of Utah (Supplemental Information).

### RIL Phenotyping

Each strain was assayed an average of 2.1 times, randomized across 14 blocks (days). Assays were performed on NGM-agarose plates, which differ from the recipe in [33] by the addition of 1.25% agarose. 40 L4 males were transferred to NGM-agarose plates seeded 1 day earlier with 50 μl OP50 *E. coli* bacteria. The males were picked from plates that had been seeded with two plugged hermaphrodites 3 days earlier, to control population density. 4 days after the 40 L4s were plated, each worm was scored for the presence of copulatory plugs on its excretory pore and elsewhere on its body (Supplemental Information). All assays were performed at 20°C.

### Quantitative Genetic Analysis

We fitted the observed counts of worms with and without plugs with a mixed-effect generalized linear model with binomial error, using the function *glmer* in R [34, 35]. Assay date and strain were included as random effects and we tested for an improvement of fit by incorporating marker genotypes as fixed effects. As a test statistic, we use the chi-square value from difference in log likelihood between the full model and a reduced model with intercept as the only fixed effect. We performed a single-QTL scan of the genome by testing multiple imputations of genotypes at 2 cM spacing as well as at the observed markers [36], taking the average chi-square value at each marker across imputations, inversely weighted by the residual deviance. Genome-wide significance thresholds were estimated by permuting the genotype vectors, preserving the original strain and date structure [37, 38]. Genome-wide thresholds at p = 0.05 were estimated from 200 permutations for each analysis.

For plotting the phenotypes in Figure 1C, we extracted estimates of each strain's plugging frequency from the random strain effect of a mixed-effect generalized linear model that incorporated assay date, as described above. The strain effects, conditional modes from the mixed-effect linear model, were extracted using the *ranef* function, and the prediction intervals are 1.96 times the standard errors derived from the posterior variances (*ranef* argument condVar = T). These values were then converted into frequencies.

Genetic correlation between Plep and Plob was tested by analyzing the Pearson correlation between the estimated strain effects.

### Trans-Plugging Assays

We set up assays with 10 L4 QG2288 (*plg-1*(N2) > QG71) males and 30 GFP-marked QG693 (*mIs12* II; *him-5* V > CB4856) males. After 4 days, we scored each worm for the Plep phenotype, blind to genotype, and then scored each worm for pharyngeal GFP to determine its genotype.

### $F_2$ Assays

$F_2$ males derived from a cross of AB2 males and CB4856 hermaphrodites and sibmating of $F_1$s were subjected to our standard 40-male 4-day assay. Individual males were then scored for excretory pore plugs and lysed for genotyping. Each worm was genotyped by PCR at an indel polymorphism at 4.057 Mb on chromosome II, close to the QTL peak at the SNP marker at 4.317 Mb (Supplemental Information). Linkage and dominance were assessed with a logistic regression including additive and dominance terms and significance was tested with a likelihood ratio test. Figure 2A plots the simple phenotypic proportions and their 95% confidence intervals calculated by normal approximation.

### Effect of Hermaphrodites

We generated vulvaless hermaphrodites by RNAi by feeding, targeting *lin-3* and *mex-3* in AB2 larvae. Knockdown of *mex-3* results in dead embryos, which prevents embryos from hatching inside their vulvaless mothers (bagging). Standard 4-day assays were set up with 40 QG71 L4 males and 1 young adult Vul hermaphrodite (Supplemental Information).

Hermaphrodite supernatant was generated by incubating ~150 QG71 hermaphrodites in 10 μl of water for an hour, then freezing and thawing the tubes. 5 μl of the supernatant was spotted on 6 cm plates prior to the addition of males. 5 μl of water was added to control plates (Supplemental Information).

We tested significance of each treatment in a logistic regression in R: anova(glm(data ~treatment, family = "binomial"), test = "LRT"), with p values estimated from the chi-square distribution.

### *dhs-28* Introgressions

We tested QG2285 (*dhs-28 (hj8)* X > QG71) and two introgression-control strains, QG2286 and QG2287 (*dhs-28* (N2) X > QG71) in standard 4-day 40-worm assays (Supplemental Information). We tested significance of each genotype in a logistic regression in R. We detected no difference in phenotype between the two control strains (p = 0.59), and we therefore pooled their data to test for an effect of *dhs-28* genotype and to plot the results in Figure 2D.

### Fine-Mapping with NILs

NILs were constructed according to the scheme in Figure S2, using visible markers *sqt-2 (sc108), mIs12,* and *dpy-2(e8)*. Phenotypes were scored in the standard 40-worm 4-day assay (Supplemental Information). These NILs narrow the QTL to the interval between 4,301,062 and 4,328,486, defined by NILs QG1448 (Plep) and QG1446 (nonPep). We subsequently used QG1451, which has a breakpoint between CB4856 and AB2 DNA in the same interval

 

as QG1446, as our nonPep NIL for comparisons with QG1448. QG1448, QG1451, and their $F_1$ male progeny were assayed in the standard assay to generate Figure 2E (Supplemental Information).

### Identifying Associated Variants

We generated Illumina sequencing data for 10 strains capable of producing copulatory plugs [9]. Reads were mapped with bwa mem (0.7.5a) [39] to the reference N2 genome (WS220) and processed with Picard (http://broadinstitute.github.io/picard/) (1.103) and samtools (http://samtools.sourceforge.net/) (0.1.18) utilities. Variants were called with the GATK HaplotypeCaller (2.6-4) [40] and filtered on mapping quality (MQ $\geq$ 40.0), depth (4 $\leq$ DP $\leq$ mean coverage × 3), read strand bias (FS $\leq$ 60.0), position within read (ReadPosRankSum $\geq -8.0$), and variant quality:depth ratio (QD $\geq$ 4.0). Regions of the 27 kb interval are highly repetitive and we were unable to make reliable calls in those regions. Genotype data are reported in the Supplemental Information (WS220 coordinates), where the causal *plep-1* variant is 4,310,427 A>T (WBVar01538101). Variant functional impact was predicted using Sift, PolyPhen, and TMHMM [41–43].

We assayed excretory pore plugging in each of these strains in triplicate 4-day assays, each including 20 L4 males of the wild isolate and 20 QX1199 males to serve as plug donors in case the wild isolate is a poor mater (Supplemental Information).

### Complementation Tests

We received a population segregating *ttTi36640*, a *Mos1* insertion in *Y52E8A.6*, from Maite Carre-Pierrat, and a population segregating *ttTi58321*, a *Mos1* insertion in *Y52E8A.4*, from Patricia Kuwabara [44]. From each population we homozygosed the insertion allele with validation by PCR.

We crossed QG1448 males with hermaphrodites of QG1448, N2, *ttTi36640*, and *ttTi58321* and picked the resulting $F_1$ L4 male progeny to set up standard 4-day 40-worm assays (Supplemental Information).

### RNAi Experiments

We inoculated LB-Ampicillin with colonies of HT115(DE3) strains carrying pL4440 (empty vector negative control) and *pY52E8A.4*$^{RNAi}$ and seeded the resulting overnight cultures on NGM-agarose plates containing IPTG and Carbenicillin [45]. We used these plates for our standard 4-day 40-male assays with strain QX1199 and QG1451 (Supplemental Information). The QX1199 L4 experiments were conducted on two dates, and we included date as an effect in the logistic regression (though it was not significant). The QX1199 experiments and QG1451 experiments were performed in single batches.

### Transcriptional Reporter Analysis

The *plep-1* transcriptional reporter comprises 1,169 bp of upstream sequence from the start codon to a HindIII site (4,313,385–4,312,216 in WS240 coordinates) amplified from N2, digested with HindIII, and cloned into HindIII/SmaI sites of pSM-GFP [46]. The reporter was injected into N2 hermaphrodites with a $P_{myo\text{-}3}$::mCherry marker (pCFJ104 [47]) to obtain multicopy array $F_1$ animals. Staged worms from two stably expressing lines (QG2465 and QG2466) were mounted on 2% agar pads in 10 μM levamisole and imaged on a Leica SP5 confocal microscope over four independent experiments.

### *plep-1* Gene Family Phylogenetics

UNC-93 domain (IPR010291) protein sequences were downloaded from Interpro (March 2014), aligned (Mafft 6.864 [48], linsi mode) and subject to Bayesian phylogenetic inference (MrBayes 3.2.2 [49]) with ten independent 4-chain runs of 10M generations (GTR model with gamma-distributed rate variation, mixed amino acid model prior).

### Male Longevity and Reproductive Success

Developmentally synchronized QG71 young adult males were placed in groups of 40 on 6 cm plates and left to mate for 3 days at 20°C. Four males, blocked according to the presence or absence of a plugged excretory pore, were placed on a 6 cm plate seeded with 150 μl of a saturated culture of OP50-GFP [50], along with eight virgin young adult *fog-2* females (hermaphrodites that cannot produce self sperm) to minimize subsequent headplugging and leaving. A total of 93 plates (47 with plugs, 46 without) were initiated. A single treatment of 50 μl 1 M KCl was added to 23 plates within each block to test for an effect of osmotic stress. Mating proceeded for 2 days at 20°C, then males were removed to fresh plates and young females were replenished (continued every 2 days thereafter to measure longevity, see below). Over the initial 2 days, mating failed for 15 of 47 plates with Plep males and 2 of 46 plates for unplugged males. The effect of KCl on mating success was not significant (Fisher's exact test, p = 0.28).

To assay longevity, males were gently prodded on the head daily and scored as dead if unresponsive. Worms dead at the plate edge due to desiccation or otherwise unaccounted for at census each day were censored. A Cox proportional hazard model was fit with the R *survival* package [51]. The main effect of initial KCl treatment on lifespan was significant and negative (p = 0.0001). The final longevity model also incorporated a suggestive interaction between Plep status and KCl treatment (marginally preferable to a model with additive effects only by likelihood ratio test, p = 0.068). All plugged males had perished by 21 days, leaving 12.7% of unplugged males alive (log 95% confidence interval 8.1%–20.1%). Raw data are in the Supplemental Information, and model fit is plotted in Figure S1.

### Wild Isolate Genotypes

To characterize the geographic distribution of the *plep-1* V278D allele, we genotyped 55 wild isolates of *C. elegans* by Illumina short-read genome sequencing or PCR-RFLP. *C. elegans* population structure is such that a random sample of strains is not a particularly meaningful concept. Our sample is enriched for strains that resemble AB2 on chromosome II, according to RAD-seq data from Andersen et al. [13], though it also includes many additional strains collected subsequent to that study. Genotypes and phenotype data for a subset of *plg-1*$^{+}$ strains are reported in the Supplemental Information.

### Hermaphrodite Activity Assays

The activity of hermaphrodites in liquid culture was assessed for three mutant strains: QG2458, a *Mos1* insertion (*ttTi53821*) in the N2 background; QG2457, an R13* nonsense point mutation (*gk140536*) in the N2 background; and QG2462, the AB2 *plep-1* locus introgressed into the N2 *him-5* background. In parallel, we assayed N2 and QG2456, an N2 derivative that controls for background effects introduced by the construction of the mutant strains (see Supplemental Experimental Procedures).

Developmentally synchronized young adult hermaphrodites were placed 10 to each well of a 96-well plate containing 100 μl of $H_2O$. A census was taken immediately and activity was scored blind over 24 hr as the number of active worms (swimming or making deep body bends) per well. Inspection at 48 hr confirmed that lack of activity at 24 hr is correlated with death.

Data were collected from 10 assays (n = 5,849 worms after limiting to wells with 7–13 worms, with mean = 10, standard deviation = 1.59; see the Supplemental Information). A binomial generalized mixed effect linear model was fit (R package *lme4* [35]) to worm activity counts per well at 24 hr with strain (or genotype as a binary variable) as fixed effect and a random assay effect. All *plep-1* mutants were significantly less active than N2 ($p < 0.01$), while the two controls strains were indistinguishable (p = 0.4).

### Gene Expression Analysis

RNA was extracted from young adult hermaphrodites (N2 and a *Mos1* insertion line, QG2458) from cultures synchronized by L1 arrest (20 hr in M9 buffer). Labeled cRNA was in vitro transcribed from 1 μg total RNA (Agilent Low Input Quick Amp Labeling Kit), hybridized to Agilent V2 4x44k microarrays against a pooled reference sample, and scanned on an Agilent G256CA Scanner (Supplemental Information). Four biological replicates and three technical replicates (after stripping microarrays by treatment with RNaseH) were hybridized. Raw data were imported into the R package limma [52, 53], background corrected (method = "normexp," offset = 50), and normalized within (method = "loess," span = 0.05) and across (method = "Gquantile") arrays. Multiple probes are present on the array for many, but not all, transcripts. We averaged over probes targeting the same set of transcript isoforms before statistical analysis, reducing the data to 22,837 probe sets for 20,143 genes. Technical replicate correlation was estimated with the function duplicateCorrelation, and differential expression for the N2-QG2458 contrast was estimated by linear model. Moderated statistics were computed with an intensity-dependent fit to prior variances, and p values were adjusted by controlling the false

discovery rate (Benjamini and Hochberg method). Processed data are in the Supplemental Information. Functional enrichments were analyzed with the Serial Pattern of Expression Levels Locator (SPELL 2.0.3r71) [54], generating rank correlation statistics against published data and testing for enrichment of gene ontology terms among the top 100 correlated genes. Gene set enrichment analysis (GSEA 2.0.14) [55] used WS234 gene ontology annotations, filtered to terms with 10–500 genes. For genes targeted by multiple probe sets, the set with the highest F-statistic was taken. FDR was estimated by permuting gene sets 10,000 times.

## ACCESSION NUMBERS

Microarray data are available from NCBI GEO under accession number GEO: GSE68351.

## SUPPLEMENTAL INFORMATION

Supplemental Information includes three figures, one table, and Supplemental Experimental Procedures and can be found with this article online at http://dx.doi.org/10.1016/j.cub.2015.09.019.

## AUTHOR CONTRIBUTIONS

L.M.N., A.S.C., D.M., M.K., M.Y., and M.V.R. designed experiments. L.M.N., A.S.C., D.M., M.K., M.Y., J.P.N., D.D.R., P.A., M.P., T.I., and M.V.R. performed experiments. L.M.N. and M.V.R. analyzed the data and wrote the paper.

## ACKNOWLEDGMENTS

This work was supported by the NIH (R01 GM089972 to M.V.R. and F32 HD065442 to A.S.C.), the Zegar Family Foundation, and New York University. We thank N. Ringstad and A. Paaby for comments and Zina Deretsky for the illustration in Figure 1B.

Received: July 29, 2015
Revised: September 7, 2015
Accepted: September 8, 2015
Published: October 8, 2015

## REFERENCES

1. Smith, J.M., and Harper, D. (2003). Animal Signals (Oxford University Press).
2. Halliday, T.R. (1983). The study of mate choice. In Mate Choice, P. Bateson, ed. (University of Cambridge), pp. 3–32.
3. Johansson, B.G., and Jones, T.M. (2007). The role of chemical communication in mate choice. Biol. Rev. Camb. Philos. Soc. *82*, 265–289.
4. Wyatt, T.D. (2003). Pheromones and Animal Behaviour (Cambridge University Press).
5. Thomas, C.G., Woodruff, G.C., and Haag, E.S. (2012). Causes and consequences of the evolution of reproductive mode in *Caenorhabditis* nematodes. Trends Genet. *28*, 213–220.
6. Garcia, L.R., LeBoeuf, B., and Koo, P. (2007). Diversity in mating behavior of hermaphroditic and male-female *Caenorhabditis* nematodes. Genetics *175*, 1761–1771.
7. Kleemann, G.A., and Basolo, A.L. (2007). Facultative decrease in mating resistance in hermaphroditic *Caenorhabditis elegans* with self-sperm depletion. Anim. Behav. *74*, 1339–1347.
8. Ting, J.J., Woodruff, G.C., Leung, G., Shin, N.-R., Cutter, A.D., and Haag, E.S. (2014). Intense sperm-mediated sexual conflict promotes reproductive isolation in *Caenorhabditis* nematodes. PLoS Biol. *12*, e1001915.
9. Palopoli, M.F., Rockman, M.V., TinMaung, A., Ramsay, C., Curwen, S., Aduna, A., Laurita, J., and Kruglyak, L. (2008). Molecular basis of the copulatory plug polymorphism in *Caenorhabditis elegans*. Nature *454*, 1019–1022.
10. Gems, D., and Riddle, D.L. (2000). Genetic, behavioral and environmental determinants of male longevity in *Caenorhabditis elegans*. Genetics *154*, 1597–1610.
11. Chasnov, J.R. (2013). The evolutionary role of males in *C. elegans*. Worm *2*, e21146.
12. Rockman, M.V., and Kruglyak, L. (2009). Recombinational landscape and population genomics of *Caenorhabditis elegans*. PLoS Genet. *5*, e1000419.
13. Andersen, E.C., Gerke, J.P., Shapiro, J.A., Crissman, J.R., Ghosh, R., Bloom, J.S., Félix, M.-A., and Kruglyak, L. (2012). Chromosome-scale selective sweeps shape *Caenorhabditis elegans* genomic diversity. Nat. Genet. *44*, 285–290.
14. Cutter, A.D., and Payseur, B.A. (2013). Genomic signatures of selection at linked sites: unifying the disparity among species. Nat. Rev. Genet. *14*, 262–274.
15. Altun, Z.F., and Hall, D.H. (2009). Excretory system. In WormAtlas, L.F. Herndon, ed. http://www.wormatlas.org/hermaphrodite/excretory/Excframeset.html.
16. Ludewig, A.H., and Schroeder, F.C. (2013). Ascaroside signaling in *C. elegans*. WormBook, 1–22.
17. Chute, C.D., and Srinivasan, J. (2014). Chemical mating cues in *C. elegans*. Semin. Cell Dev. Biol. *33*, 18–24.
18. Butcher, R.A., Ragains, J.R., Li, W., Ruvkun, G., Clardy, J., and Mak, H.Y. (2009). Biosynthesis of the *Caenorhabditis elegans* dauer pheromone. Proc. Natl. Acad. Sci. USA *106*, 1875–1879.
19. de la Cruz, I.P., Levin, J.Z., Cummins, C., Anderson, P., and Horvitz, H.R. (2003). *sup-9, sup-10*, and *unc-93* may encode components of a two-pore K+ channel that coordinates muscle contraction in *Caenorhabditis elegans*. J. Neurosci. *23*, 9133–9145.
20. Saifee, O., Wei, L., and Nonet, M.L. (1998). The *Caenorhabditis elegans unc-64* locus encodes a syntaxin that interacts genetically with synaptobrevin. Mol. Biol. Cell *9*, 1235–1252.
21. Barrière, A., and Félix, M.-A. (2005). High local genetic diversity and low outcrossing rate in *Caenorhabditis elegans* natural populations. Curr. Biol. *15*, 1176–1184.
22. Félix, M.-A., and Duveau, F. (2012). Population dynamics and habitat sharing of natural populations of *Caenorhabditis elegans* and C. *briggsae*. BMC Biol. *10*, 59.
23. Chasnov, J.R., So, W.K., Chan, C.M., and Chow, K.L. (2007). The species, sex, and stage specificity of a *Caenorhabditis* sex pheromone. Proc. Natl. Acad. Sci. USA *104*, 6730–6735.
24. Lipton, J., Kleemann, G., Ghosh, R., Lints, R., and Emmons, S.W. (2004). Mate searching in *Caenorhabditis elegans*: a genetic model for sex drive in a simple invertebrate. J. Neurosci. *24*, 7427–7434.
25. Huang, C.G., Lamitina, T., Agre, P., and Strange, K. (2007). Functional analysis of the aquaporin gene family in *Caenorhabditis elegans*. Am. J. Physiol. Cell Physiol. *292*, C1867–C1873.
26. Teramoto, T., Lambie, E.J., and Iwasaki, K. (2005). Differential regulation of TRPM channels governs electrolyte homeostasis in the *C. elegans* intestine. Cell Metab. *1*, 343–354.
27. Rockman, M.V., Skrovanek, S.S., and Kruglyak, L. (2010). Selection at linked sites shapes heritable phenotypic variation in *C. elegans*. Science *330*, 372–376.
28. Cutter, A.D., and Payseur, B.A. (2003). Selection at linked sites in the partial selfer *Caenorhabditis elegans*. Mol. Biol. Evol. *20*, 665–673.
29. Srinivasan, J., Kaplan, F., Ajredini, R., Zachariah, C., Alborn, H.T., Teal, P.E.A., Malik, R.U., Edison, A.S., Sternberg, P.W., and Schroeder, F.C. (2008). A blend of small molecules regulates both mating and development in *Caenorhabditis elegans*. Nature *454*, 1115–1118.
30. Morsci, N.S., Haas, L.A., and Barr, M.M. (2011). Sperm status regulates sexual attraction in *Caenorhabditis elegans*. Genetics *189*, 1341–1346.

 

31. Markert, M., and García, L.R. (2013). Virgin *Caenorhabditis* remanei females are attracted to a coital pheromone released by con-specific copulating males. Worm *2*, e24448.
32. Wang, J., Silva, M., Haas, L.A., Morsci, N.S., Nguyen, K.C.Q., Hall, D.H., and Barr, M.M. (2014). *C. elegans* ciliated sensory neurons release extracellular vesicles that function in animal communication. Curr. Biol. *24*, 519–525.
33. Stiernagle, T. (2006). Maintenance of *C. elegans*. WormBook, 1–11.
34. R Core Team. R: A Language and Environment for Statistical Computing. http://www.R-project.org/.
35. Bates, D.M. (2010). lme4: Mixed-effects modeling with R. http://lme4 r-forge r-project org/book.
36. Sen, S., and Churchill, G.A. (2001). A statistical framework for quantitative trait mapping. Genetics *159*, 371–387.
37. Churchill, G.A., and Doerge, R.W. (1994). Empirical threshold values for quantitative trait mapping. Genetics *138*, 963–971.
38. Churchill, G.A., and Doerge, R.W. (2008). Naive application of permutation testing leads to inflated type I error rates. Genetics *178*, 609–610.
39. Li, H., and Durbin, R. (2010). Fast and accurate long-read alignment with Burrows-Wheeler transform. Bioinformatics *26*, 589–595.
40. McKenna, A., Hanna, M., Banks, E., Sivachenko, A., Cibulskis, K., Kernytsky, A., Garimella, K., Altshuler, D., Gabriel, S., Daly, M., and DePristo, M.A. (2010). The Genome Analysis Toolkit: a MapReduce framework for analyzing next-generation DNA sequencing data. Genome Res. *20*, 1297–1303.
41. Ng, P.C., and Henikoff, S. (2003). SIFT: Predicting amino acid changes that affect protein function. Nucleic Acids Res. *31*, 3812–3814.
42. Adzhubei, I.A., Schmidt, S., Peshkin, L., Ramensky, V.E., Gerasimova, A., Bork, P., Kondrashov, A.S., and Sunyaev, S.R. (2010). A method and server for predicting damaging missense mutations. Nat. Methods *7*, 248–249.
43. Krogh, A., Larsson, B., von Heijne, G., and Sonnhammer, E.L. (2001). Predicting transmembrane protein topology with a hidden Markov model: application to complete genomes. J. Mol. Biol. *305*, 567–580.
44. Vallin, E., Gallagher, J., Granger, L., Martin, E., Belougne, J., Maurizio, J., Duverger, Y., Scaglione, S., Borrel, C., Cortier, E., et al. (2012). A genome-wide collection of *Mos1* transposon insertion mutants for the *C. elegans* research community. PLoS ONE *7*, e30482.
45. Ahringer, J. (2006). Reverse genetics. WormBook, 1–43.
46. McGrath, P.T., Rockman, M.V., Zimmer, M., Jang, H., Macosko, E.Z., Kruglyak, L., and Bargmann, C.I. (2009). Quantitative mapping of a digenic behavioral trait implicates globin variation in *C. elegans* sensory behaviors. Neuron *61*, 692–699.
47. Frøkjaer-Jensen, C., Davis, M.W., Hopkins, C.E., Newman, B.J., Thummel, J.M., Olesen, S.-P., Grunnet, M., and Jorgensen, E.M. (2008). Single-copy insertion of transgenes in *Caenorhabditis elegans*. Nat. Genet. *40*, 1375–1383.
48. Katoh, K., Kuma, K., Toh, H., and Miyata, T. (2005). MAFFT version 5: improvement in accuracy of multiple sequence alignment. Nucleic Acids Res. *33*, 511–518.
49. Ronquist, F., and Huelsenbeck, J.P. (2003). MrBayes 3: Bayesian phylogenetic inference under mixed models. Bioinformatics *19*, 1572–1574.
50. Labrousse, A., Chauvet, S., Couillault, C., Kurz, C.L., and Ewbank, J.J. (2000). *Caenorhabditis elegans* is a model host for *Salmonella typhimurium*. Curr. Biol. *10*, 1543–1545.
51. Therneau, T.M., and Grambsch, P.M. (2010). Modeling Survival Data: Extending the Cox Model (Springer).
52. Smyth, G.K. (2004). Linear models and empirical bayes methods for assessing differential expression in microarray experiments. Stat. Appl. Genet. Mol. Biol. *3*, e3.
53. Ritchie, M.E., Silver, J., Oshlack, A., Holmes, M., Diyagama, D., Holloway, A., and Smyth, G.K. (2007). A comparison of background correction methods for two-colour microarrays. Bioinformatics *23*, 2700–2707.
54. Hibbs, M.A., Hess, D.C., Myers, C.L., Huttenhower, C., Li, K., and Troyanskaya, O.G. (2007). Exploring the functional landscape of gene expression: directed search of large microarray compendia. Bioinformatics *23*, 2692–2699.
55. Subramanian, A., Tamayo, P., Mootha, V.K., Mukherjee, S., Ebert, B.L., Gillette, M.A., Paulovich, A., Pomeroy, S.L., Golub, T.R., Lander, E.S., and Mesirov, J.P. (2005). Gene set enrichment analysis: a knowledge-based approach for interpreting genome-wide expression profiles. Proc. Natl. Acad. Sci. USA *102*, 15545–15550.